Applied Biochemistry and Biotechnology (2025) 197:6640–6658
https://doi.org/10.1007/s12010-025-05336-8

ORIGINAL ARTICLE

Synthesis, Characterization, and Potential Applications of Menthol-Amino Acid Ester Derivatives

Lolakhon Ettibaeva[1] · Abduaziz Ergashev[1] · Ugilay Abdurakhmanova[1] · Ruhan Benlikaya[2] · Pınar Güner[3] · Alimjan Matchanov[4]

Accepted: 27 June 2025 / Published online: 6 August 2025

Abstract

This study focuses on the synthesis of menthyl ester derivatives from menthol and various amino acids such as glycine, histidine, and leucine, and their characterization via high-performance liquid chromatography, Fourier-transform infrared (FTIR) spectroscopy, carbon-13 nuclear magnetic resonance (^{13}C-NMR) spectroscopy, X-ray diffraction (XRD), and scanning electron microscopy (SEM) analyses to determine their structural, chemical, and morphological properties. The FTIR and ^{13}C-NMR analyses provided detailed information about the molecular structure, confirming the formation of the menthol-amino acid ester derivatives. The XRD and SEM analyses revealed distinct crystal structures and surface morphologies of the menthol and the ester derivatives. Additionally, antimicrobial activity tests were performed to evaluate their effectiveness against various microorganisms. This study highlights the potential of these compounds as promising candidates for innovative applications in antimicrobial therapies and related scientific disciplines.

Keywords Menthol · Amino acid · Menthyl ester · Antimicrobial activity · Terpenoid · Antioxidant

Introduction

Plants remain the most exclusive source of medicines, even after the Industrial Revolution and the invention of organic chemistry. According to the World Health Organization (WHO), traditional medicines and therapies are used by 80% of the world's population [1]. Approximately 25% of the medicines currently administered around the world are derived

✉ Ruhan Benlikaya
ruhan@balikesir.edu.tr

[1] Department of Chemistry, Gulistan State University, Gulistan, Uzbekistan

[2] Department of Secondary Science and Mathematics Education, Balıkesir University, Balıkesir, Turkey

[3] Department of Biology, Balıkesir University, Balıkesir, Turkey

[4] Institute of Bioorganic Chemistry named after A. Sadikov, Tashkent, Uzbekistan

from natural resources. According to WHO research, 11% of these drugs are purely plant-based, while a significant proportion is synthetic drugs made from natural precursors. Natural chemicals can serve as lead compounds, facilitating the rational design and development of innovative drugs, biomimetic synthesis, and identification of previously undiscovered medicinal properties [2]. The use of natural products, especially those derived from plants, for medicinal purposes and alternative therapies has recently gained popularity. The lack of efficacy of conventional drugs, abuse of synthetic drugs, side effects, and toxicity issues are some of the factors driving interest in plant-derived drugs [3].

Terpenoids such as menthol and taxol show many biological effects and are often used in traditional medicine and pharmaceutical research [4]. The medicinal properties are related to the presence of phenolic chemicals in mint species. Menthol, which is a cyclic monoterpene alcohol of plant origin, is isolated from peppermint or other mint oils. It is also commonly used in oral hygiene products, pesticides, cosmetics, pharmaceuticals, confectionery, and flavoring agents because of its antioxidant, anti-inflammatory, and analgesic effects [5]. Menthol is widely used in a variety of diseases, including inflammatory diseases, cancer, pain disorders, respiratory disorders, cardiovascular diseases, and skin diseases due to its numerous biological properties. Research on novel menthol-based biomaterials, which are undervalued anticancer agents, is warranted to expand their traditional uses, especially to provide better formulations containing additional active molecules, to reduce drug toxicity, and to develop structurally optimized analogs, which require more extensive and interdisciplinary efforts [6].

Enhancing the properties of menthol above through structural modification can lead to the development of more effective derivatives. In the review of de Castro Teixeira et al. [7], 26 articles on in vitro studies were selected, including 62 potential antifungal menthol compounds obtained by organic synthesis. The number of studies conducted on menthyl esters, a group of these compounds, has begun to increase over the past 5 years [8–13].

Menthyl esters with dicarboxylic acids synthesized by Ettibaeva et al. were examined with respect to their physical and chemical properties [8, 9]. Novel derivatives such as dimenthyl succinate, menthyl maleinate, menthyl malonate, and dimenthyl glutarate were synthesized, and their biological activities were evaluated [8]. The potential of menthol−amino acid conjugates synthesized by the reaction of L-menthol with t-Boc−amino acids as TRPM8 agonists was described [10]. The study investigated in silico design and synthesis of new menthol ester derivatives to synthesize potent antibacterial and anti-inflammatory medicines [11]. The developed menthyl esters of valine and isoleucine were found to exhibit anti-inflammatory properties beyond those of the well-known menthol in macrophages stimulated with lipopolysaccharide and in a mouse model of colitis induced by sodium dextran sulfate [12]. The study by Tsuzuki et al. [13] focused on developing novel compounds, specifically terpene derivatives consisting of menthol and various amino acids, with the potential to elicit plant defense responses. Menthyl esters of glycine, alanine, valine, leucine, isoleucine, and phenylalanine were prepared by esterifying L-menthol with the amino acids using the method based on a previous report, and characterized using ^{1}H-NMR spectroscopy. Among the tested menthyl esters, valine menthyl ester (ment-VaI) was found to be particularly effective in elevating the transcript levels of defense genes in soybean plants. Menthol and the menthyl esters of glycine, alanine, leucine, isoleucine, and phenylalanine were not effective at inducing these defense genes at the same dose (1 μM). The study also found that both menthol and ment-Val were effective in reducing the number of eggs laid by adult female two-spotted spider mites (*Tetranychus urticae*) on leaves.

More studies on menthol derivatives are needed to better explore their biological activity and confirm their efficacy. This should be done without ruling out chemical structure

modification as a way to improve pharmacological potential [7]. The aim of this study is to synthesize menthol-amino acid ester derivatives through the reaction of menthol with various amino acids such as glycine, histidine, and leucine, and to characterize these compounds in respect of chemical, structural, and morphological properties. Moreover, the investigation of the antimicrobial potential of these compounds and the assessment of their applicability in the development of novel antimicrobial agents constitute the main motivation of this study.

Materials and Methods

Chemicals

All reagents and solvents used in the synthesis were of analytical grade. Menthol was purchased from Shandong Baovi Energy Technology Co., Ltd. L-Histidine and L-leucine were obtained from Xi'an Ceres Biotech Co., Ltd. Glycine was purchased from Wuxi Jinghai Amino Acid Co., Ltd. Sabouraud dextrose broth (SDB) and dimethyl sulfoxide (DMSO) were from Merck. Mueller Hinton broth (MHB) was obtained from Millipore. Thiazolyl blue tetrazolium bromide (TBTB), methanol, and ethanol were acquired from Sigma.

Synthesis of Menthol-Amino Acid Ester Derivatives

0.013 mol of the menthol was dissolved in 0.5 mL of methanol by stirring for 30 min. 0.01 mol of each amino acid (glycine (Gly), leucine (Leu), and histidine (His)) was thoroughly dissolved in 7 mL of concentrated HCl. After both solutions were completely dissolved, they were combined into a single container, and then stirred at 35–40 °C for 5–6 h. The resulting mixtures were washed with cold ethanol and dried in vacuum to obtain the menthol-based compounds shown in Fig. 1. The percent yields of Ment-Gly, Ment-Leu, and Ment-His compounds were determined as 85.2%, 93.2%, and 76.1%, respectively.

Characterization

High-performance liquid chromatography (HPLC), Fourier-transform infrared spectroscopy (FTIR), X-ray diffraction (XRD), carbon-13 nuclear magnetic resonance (^{13}C-NMR) spectroscopy, and scanning electron microscopy (SEM) analyses were used to clarify chemical structures and surface morphologies of the menthol and its ester derivatives with the amino acids. In addition, broth dilution method was used to examine antimicrobial

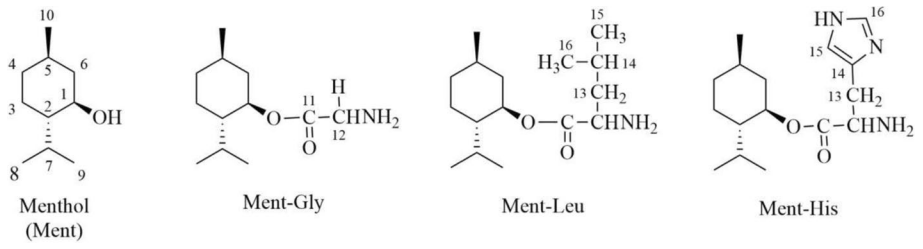

Fig. 1 Structures of the ester derivatives formed by menthol with the amino acids

activity of each compound. All the methods above provide detailed insights into the structures of the menthol-amino acid ester derivatives, which is critical for evaluating their efficacy and safety as pharmaceutical agents.

HPLC Analyses

HPLC was performed using a Shimadzu LC-40D system from Japan to purify and separate the menthol and the ester derivatives. The separation was carried out on Shim-pack Scepter C18-120 column in Agilent 1200 HPLC system (Agilent Technologies, USA). The column measures 250 mm in length and 4.6 mm in internal diameter, with a particle size of 3 µm. Silica gel 60 F254 thin-layer chromatography plates were used as the stationary phase. Each compound was dissolved at a concentration of 5 mg/mL in ethanol or methanol. The mobile phase was a mixture of water and acetonitrile, and its composition changed over time according to a gradient program: From 0.0 to 3.0 min, the mobile phase was 20% water and 80% acetonitrile. From 4.0 to 7.0 min, it changed to 70% water and 30% acetonitrile. From 8.0 to 10.0 min, it shifted to 40% water and 60% acetonitrile. The mobile phase returned to the initial condition of 20% water and 80% acetonitrile at 11.0 min. The flow rate of the mobile phase was set at 0.8 mL/min, and the column temperature was maintained at 30 °C to ensure consistent separation conditions. Detection of the compounds was carried out using a refractive index detector (RID-20A), which measures changes in the refractive index of the mobile phase as different compounds elute from the column.

FTIR Analyses

FTIR analyses were performed with the attenuated total reflection mode of IR Affinity-1S (Shimadzu, Japan) spectrometer. The analyses with the resolution of 2 cm^{-1} were conducted in the range of 550–4000 cm^{-1}.

^{13}C-NMR Analyses

^{13}C-NMR measurements were conducted on an Agilent Technologies brand 400 MHz NMR spectrometer. The samples were measured at 298 K in DMSO-d_6 (Deutero GmbH, Kastellaun, Germany) with reference to the residual deuterated solvent signal (δ_C 39.5 ppm). Signal splitting patterns were described as singlet (s), doublet (d), multiplet (m), and doublet of triplets (dt).

XRD Analyses

XRD patterns were obtained via a Rigaku Ultima-IV X-ray diffraction device. The X-ray beam was derived from nickel-filtered Cu Kα ($\lambda = 0.154$ nm) radiation in a sealed tube operated at 40 kV and 15 mA. The diffraction curves were ranged from 2 to 60° at a scan speed of 5°/min.

SEM Analyses

Surface morphologies of the compounds were examined via a QUANTA 400 F field emission SEM with a resolution of 1.2 nm after they were coated with Au–Pd (3 nm) on a

carbon film. SEM images were obtained from the surface of each compound at × 10,000 and × 20,000 magnifications.

Antimicrobial Activity Tests

To evaluate the antimicrobial activity of the compounds, various Gram (+) bacteria (*Staphylococcus aureus* (*ATCC 6538P*), *Bacillus cereus* (*CCM 99*), and *Streptococcus agalactiae* (*ATCC 23956*)) and Gram (−) bacteria (*Klebsiella pneumoniae* (*CCM 26 2318*), *Escherichia coli* (*ATCC 11230*), *Proteus vulgaris* (*ATCC 6897*), and *Serratia marcescens* (*ATCC 13880*)) were used. Furthermore, the fungal pathogen *Candida albicans* (ATCC10239) was also utilized in this study.

For the evaluation of antimicrobial properties, various methods such as broth dilution method [14, 15], disk diffusion method [15–18], conductivity determination [14], determination of intracellular adenine nucleoside triphosphate [14], and biofilm inhibition potential assay [16] have been utilized. The broth dilution method is the standard method used to determine minimum inhibitory concentration (MIC) and minimum bactericidal/fungicidal concentration (MBC/MFC) values. Considering MIC and MBC values together provides more detailed and quantitative information regarding the effectiveness of an antimicrobial agent against bacteria. MBC values specifically indicate the concentration required to kill bacteria, whereas MIC values indicate the concentration that inhibits visible growth. Other methods, such as the disk diffusion method, generally offer a qualitative or semi-quantitative assessment of efficacy by measuring only the diameter of the inhibition zone. The study by Huang et al. [14] indicated that MIC and MBC values were examined for *further* evaluation of antibacterial properties after the disk diffusion test, implying a more comprehensive assessment than disk diffusion alone. The MIC values were determined for ZnO nano-flowers [15], and the efficacy of the nano-flowers synthesized by different methods was compared using the quantitative values. Similarly, MIC and MBC values were determined for silver nanoparticles, and these values were used to interpret the agent's "outstanding antimicrobial activity." Lower MIC and MBC values indicated higher potency of the agent [14, 15]. This combined approach offers quantitative, concentration-based results, clarifying whether the effect is primarily inhibitory or killing. Furthermore, it allows for a direct comparison of potency at the concentration level. These features are what distinguish the combined use of MIC and MBC/MFC from the methods that only measure inhibition zones.

MIC values for the microorganisms mentioned above were determined using the dilution methods according to Approved Standards [19, 20] for antimicrobial susceptibility tests. MHB and SDB were used for antibacterial activity and antifungal activity, respectively. For the antimicrobial activity studies, each sample was dissolved in DMSO to prepare a stock solution at a concentration of 1024 µg/mL. The final concentrations in the wells ranged from 1 to 512 µg/mL. In this study, the negative control well contained no organisms, whereas the positive control well contained organisms. The antibacterial and antifungal activity tests were performed in three series. All microplates were incubated at 37 °C for the bacteria and 28 °C for the fungus during 24 h. Subsequently, 20 µL of TBTB was added to the wells and incubated for 4 h more at 37 °C. The color change in the solution indicated positive growth, with the wells showing this change turning pink. For the determination of MBC and MFC values, an inoculum was taken from the wells at the MIC and higher-concentration and then added to the wells containing fresh and sterile SDB for the fungus and MHB for the bacteria. The plates were then incubated as before, at 37 °C

for the bacteria and at 28 °C for the fungus. The color change in the positive and negative control wells was checked with the TBTB indicator. The MBC/MFC values were determined as the lowest concentrations without bacterial or fungal growth.

Results and Discussion

HPLC Analyses

HPLC chromatograms of the menthol and its compounds are shown in Fig. 2. The retention time is approximately 4.30 min in the chromatogram of the menthol. The retention times of Ment-His, Ment-Gly, and Ment-Leu are 11.98, 8.69, and 6.33 min, respectively. The typical retention times of L-menthol assigned the (1R, 2S, 5R) configuration, dodecanoic acid, and their ester (L-menthyl dodecanoate) were determined in another study [21] to be 5.6, 9.3, and 18.3 min, respectively. The effects of the functional groups in the amino acids on the polarity of the compounds can alter the separation process in HPLC. The observed changes in the retention times indicate the presence of new menthol compounds. In addition, the width and height of the peaks for each compound in Fig. 2 are clear and distinct, indicating the purity of the substances obtained. This also confirms the absence of additional impurities.

The retardation factor (Rf) value is the ratio of the distance traveled by a compound (cm) to that traveled by a solvent (cm). The Rf values of the menthol, Ment-Gly, Ment-Leu, and Ment-His were determined to be 0.55, 0.45, 0.5, and 0.4 cm, respectively. The Rf values of Ment-Gly and Ment-His are lower than those of the others due to the functional groups of the amino acids increasing the polarity of the compounds. Ment-His has the lowest Rf value due to the presence of an imidazole ring, which makes it highly polar. The Rf value of Ment-Leu is slightly greater than that of Ment-Gly because of the nonpolar alkyl chain of leucine which interacts less with the adsorbent. The comparison of these R_f values confirm the formation of new menthol-based compounds.

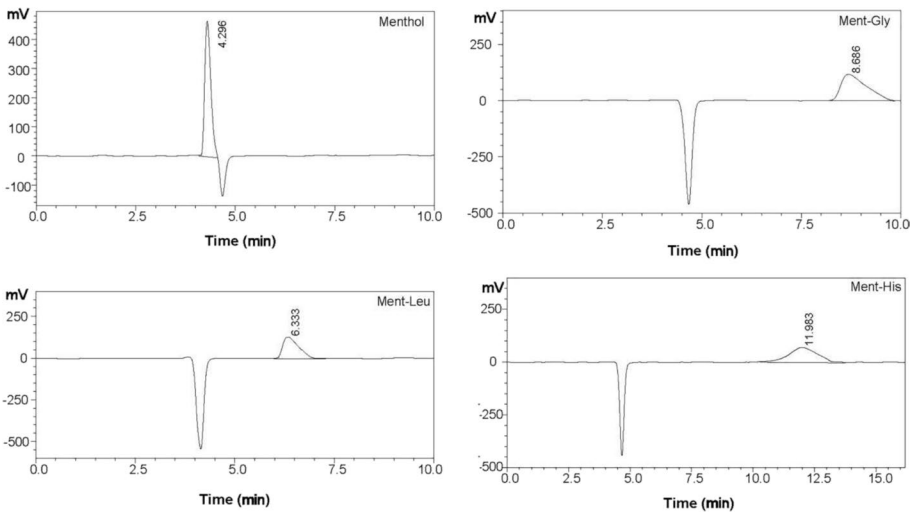

Fig. 2 HPLC chromatograms of the menthol, Ment-Gly, Ment-Leu, and Ment-His compounds

FTIR Analyses

The FTIR spectra of the menthol and its compounds are shown in Fig. 3. In the FTIR spectrum of the menthol (Fig. 3a), a broad peak is observed at around 3246 cm^{-1}, corresponding to OH stretching (H-bonded). The C–H stretching exhibits several distinct peaks in the range of 2800–3000 cm^{-1} due to the stretching vibrations of methyl (-CH_3) and methylene (> CH_2). The C–O group displays stretching vibrations in the range of 1000–1300 cm^{-1}. Additionally, the bending vibrations are observed in the range of 1300–1500 cm^{-1}, corresponding to the bending of the methyl and methylene groups. These observations are consistent with those of another studies [10, 22].

The changes in the ranges of 3000–3300 cm^{-1}, 2800–3000 cm^{-1}, and 1700–1750 cm^{-1} indicate the presence of –NH_2, –CH_2, and –COO groups arised from the reaction of the menthol with the glycine in the FTIR spectrum of Ment-Gly compound (Fig. 3b), respectively. In addition, the peaks at 848 cm^{-1} (C-N stretch) and at 1213 cm^{-1} (C–C-O stretch) also confirm the functional groups. The FTIR spectra of Ment-Leu and Ment-His compounds in Fig. 3c–d show similar changes mentioned above, as the functional groups of leucine and histidine reacting with menthol are similar to that in glycine. In addition, Ment-His may have peaks at 815, 1221, and 1391 cm^{-1} due to the imidazole group of histidine [23–25] in its FTIR spectrum. The lack of the characteristic –OH stretching of menthol at 3246 cm^{-1} and the appearance of carbonyl (C = O) stretching in the range of 1730–1736 cm^{-1} in the FTIR spectra (Fig. 3b–d) reveal that the hydroxyl group of the menthol reacted with the carboxyl groups of the amino acids to form the menthyl ester derivatives, as supported by another studies [10, 26].

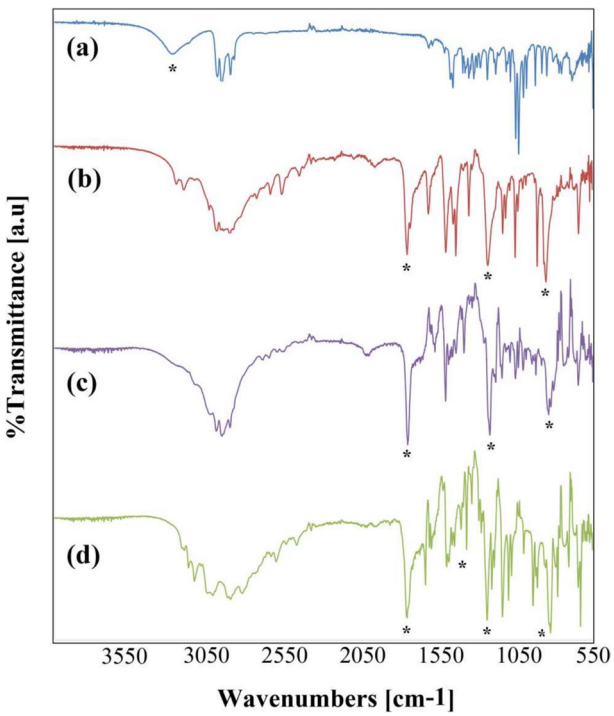

Fig. 3 FTIR spectra of the menthol (**a**), Ment-Gly (**b**), Ment-Leu (**c**), and Ment-His (**d**)

C-NMR Analyses

The ^{13}C chemical shifts from the ^{13}C-NMR spectra (*see Supplementary Information, SI* Figs. 1, 2, 3, 4) of the menthol and its compounds are summarized in Table 1. Some of the observed shifts in the spectrum of the menthol and possible carbon atoms indicated by those shifts are largely in agreement with the results of the spectrum in which DMSO-d_6 was used as a solvent in another study [27]. The consistent results with the study are shown in Table 1 in italics. The chemical shifts for the carbon atoms numbered with 1 and 2 in Fig. 1 were reported as 70.24 and 50.40 ppm, whereas 70.80 and 50.80 ppm values are observed for these carbons in this study. Ment-Gly, Ment-Leu, and Ment-His compounds have chemical shifts between 169 and 173 ppm for the ester carbon (11) and between 40 and 53 ppm for the carbon (12). The shifts for the carbon atoms (11) and (12) at various amino esters of menthol [28] were observed in the ranges of 166.9–170.9 ppm and 40.7–60.6 ppm, respectively. These shifts in this study are in line with that of the study. In addition, the chemical shifts for the carbons (11), (16), (14), and (15) were observed at approximately 175, 140, 130, and 120 ppm in the ^{13}C-NMR spectra of polycrystalline powders of histidine, respectively [29]. The chemical shifts of Ment-His for these carbons are consistent with the study. These observations support the findings obtained from the FTIR analysis and possible reaction schemes for the synthesis of the menthol-amino acid ester derivatives in Fig. 4.

XRD Analyses

The thermodynamic behavior of menthol under variable temperature and pressure conditions reveals complex phase equilibria involving multiple solid-state forms. Menthol stands out for its diverse crystallization and melting behaviors. It crystallizes in at least four forms (α, β, γ, δ), but only the α form is stable, melting at 42.5 °C. The other forms are unstable (monotropic) with lower melting points and eventually transform into the stable α form over time [30]. In addition, menthol of a single asymmetric carbon atom exists as two distinct optical isomers: the levorotatory enantiomer (L-menthol) and the dextrorotatory enantiomer (D-menthol). The predominant form encountered naturally is L-menthol, which is commonly isolated from *Mentha* species, such as *M. piperita*. Conversely, D-menthol is predominantly produced via chemical synthesis and can serve as a replacement or supplement for naturally derived menthol. DL-menthol, widely utilized across various industrial fields, is defined as a racemic mixture comprising equimolar proportions of the L- and D-menthol enantiomers [31]. The study of Corvis et al. [31] reported that it was not possible to determine the crystal structure of the racemic menthol from powder diffraction patterns using Rietveld refinement. The crystal structure of this compound was subsequently determined by X-ray single crystal diffraction. It was noted that the hydrogen atom of the hydroxyl group was shared by two independent menthol units. This complex structure is thought to explain the difficulty in obtaining the crystal structure from the powder diffraction pattern. The metastable (β) polymorphs of L- and DL-menthol were identified, and their cell parameters were determined using X-ray powder diffraction. It was also stated that β L-menthol remained stable at − 80 °C for at least 8 h. β DL-menthol rapidly converted to its stable form (α form) at 15 °C [31]. The presence of various polymorphic forms and the distinct crystalline forms in menthol and the operating conditions resulted in different patterns in XRD analyses [31, 32]. In addition, the standard menthol crystals produced by the conventional method showed well-defined crystalline peaks with 2θ equals to 9.24,

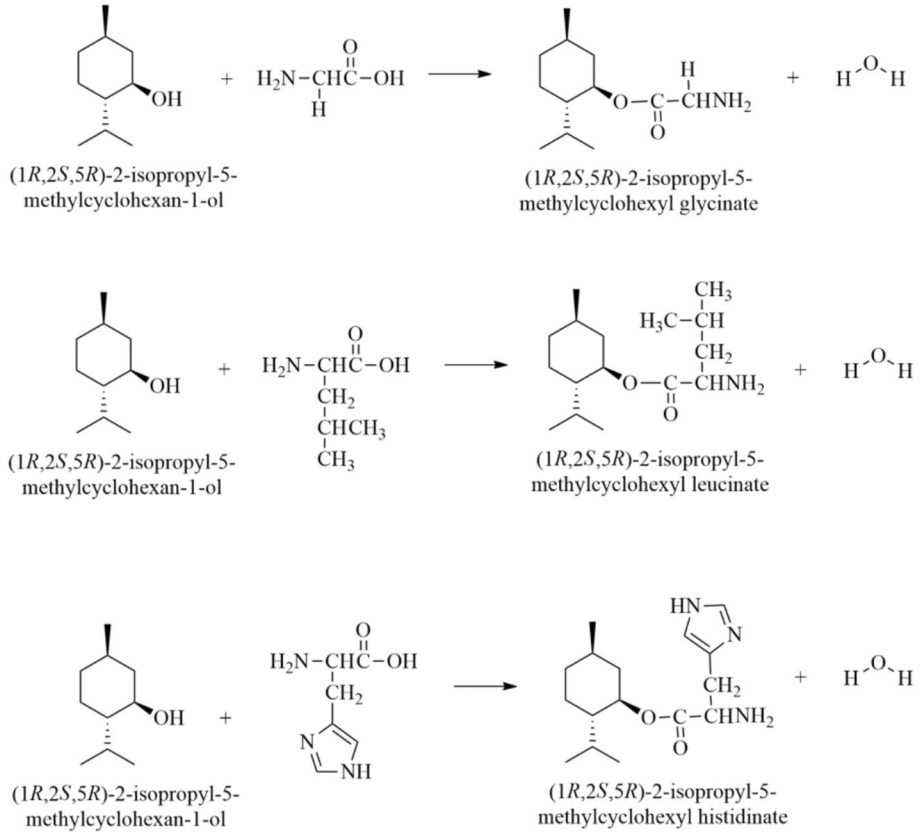

Fig. 4 Possible reaction schemes for the synthesis of the menthol-amino acid ester derivatives

13.93, 22.19, 52.26, and 57.46°, while the menthol crystals prepared via short-path molecular fractional distillation followed by stripping crystallization exhibited the peaks with 2θ equals to 8.01, 14.15, 15.24, 16.76, 17.38, 19.21, 20.35, and 21.73° [22]. These findings also show that the synthesis method affects the crystal structure of the resulting menthol and, consequently, its XRD pattern.

The peak values observed for menthol in some studies [22, 31, 32], along with the limitations mentioned above regarding its XRD analysis, were examined to evaluate the XRD pattern of menthol in this study. The sharpest five peaks in the XRD pattern, ranging from 2θ = 6 to 24°, at 25 °C for α L-menthol, were approximately at 8, 16.8, 17.3, 19.2, and 20.5°. Additionally, the peaks of moderate and weak intensity were also observed in this pattern [31]. In order to examine the effect of biofield energy on the physical and structural properties of thymol and menthol, the control and the biofield-treated menthol samples were characterized using XRD, DSC, TGA, and FTIR analysis techniques in the study of Trivedi et al. [33]. The control menthol sample showed the peaks with 2θ equals to 12.11, 12.33, 13.83, 14.09, 14.41, 16.07, 16.21, 16.64, 16.78, 16.93, 20.56, 20.82, 24.38, and 32.74°. Figure 5 shows the XRD patterns of the menthol, Ment-Gly, Ment-Leu, and Ment-His from bottom to top. The peaks with 2θ equals to about 8.7, 12.9, 14.7, 16.9, 17.6, 20.8, 21.2, 22.3, 26.9, and 29.5° are observed in the XRD pattern of

Table 1 ^{13}C chemical shifts of the menthol, Ment-Gly, Ment-Leu and Ment-His

Compounds	δC (ppm)	Number of atoms (Fig. 1)
Menthol	*70.80* (s), 69.41 (s)	1
	50.80 (s), 46.85 (d), 45.83 (s), 44.54 (s)	2, 6
	34.44 (d), 32.45 (s), 31.19 (s)	4.5
	26.32 (s), 24.92 (d), 24.48 (d)	7
	23.55 (s), 22.94 (m),	3
	22.19 (m), 21.00 (m)	9, 10
	17.36 (m), 16.07 (m), 14.99 (s)	8
Ment-Gly	169.37 (s),	11
	41.61 (s), 40.85 (s)	12
	39.11 (s), 38.74 (s)	
Ment-Leu	172.04 (dt),	11
	51.79 (d), 50.45 (s)	12
	39.68 (s), 38.60 (s)	13, 14
	24.86 (s), 23.45 (s), 22.18 (s)	15, 16
Ment-His	170.25 (s)	11
	135.74 (s), 135.68 (s), 133.56 (s), 133.49 (s)	16, 14
	127.75 (s), 119.50 (s), 117.53 (s)	15
	52.34 (s), 50.90 (s)	12
	39.30 (s)	13
	27.06 (s), 25.73 (s), 24.41 (s)	

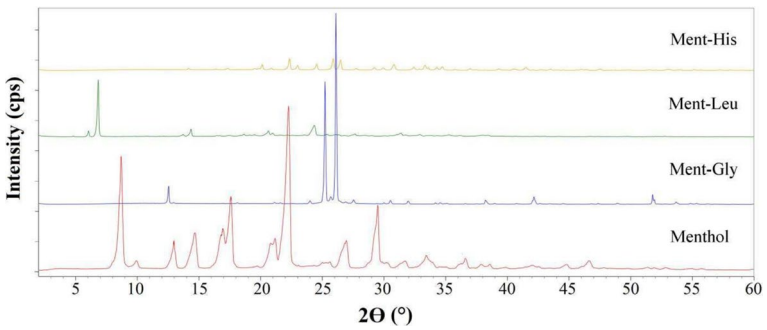

Fig. 5 XRD patterns of the menthol, Ment-Gly, Ment-Leu, and Ment-His

the menthol as well as some weak peaks with lower heights than the peaks above. These peaks are not expected to be completely consistent with the data in the literature due to the reasons mentioned above. Additionally, the XRD data obtained for menthol in this study show similarities with the findings reported by Corvis et al. [31] and Mushtaq et al. [22] in terms of some peaks. Considering the phase transitions of menthol above, the observed peaks, and the variability in the peak widths in Fig. 5, it may be said that there are probably phase transitions and multiple phases in the structure of the menthol. The peaks of the menthol disappeared in the XRD patterns of its compounds. In addition, Ment-Gly has

two sharp peaks at 25.2 and 26.1°, whereas Ment-Leu has a sharp peak at 6.85° according to its XRD pattern. Ment-His's pattern shows no peak with an intensity as high as those observed for other compounds. However, the peaks with 2θ values of about 22.3, 25.9, and 26.4° are the three most intense peaks for this compound. According to the XRD findings, each compound has a unique crystal structure that differs from that of the menthol.

The detailed analysis and the crystallite sizes for the prominent peaks at the XRD patterns in Fig. 5 are summarized in Table 2. The average crystallite size is found to be 23.8 nm with a standard deviation of 9.17 nm when the peaks at Table 2 are included in the calculation of the crystallite sizes in the menthol by using Scherrer equation. The average values, calculated using this equation, were reported as 45.08 nm and 52.23 nm for menthol samples in another studies [22, 33]. The values for Ment-Gly, Ment-Leu, and Ment-His compounds are 86.4 ± 7.11 nm, 50.37 ± 21.70 nm, and 56.76 ± 9.67 nm, respectively. It can be said that all compounds have nanocrystalline structures. In addition, it can be concluded that the average crystallite sizes of the menthol compounds are larger than that of the menthol.

SEM Analyses

The mint essential oil obtained through short-path molecular fractional distillation in another study [22] yielded fractions of 5.9 g at 21–23 °C (F1), 4.6 g at 32–35 °C (F2),

Table 2 Detailed XRD analysis for the compounds

Compound	2Θ (°)	d (Å)	Height (cps)	FWHM (°)	Int. I (cps°)	Crystallite size d (nm)
Menthol	8.706	10.148	230455	0.242	66727	34.4
	12.976	6.8170	71066	0.189	28580	44.2
	14.717	6.014	74996	0.532	44075	15.7
	16.960	5.2235	78953	0.520	48503	16.1
	17.613	5.0315	152737	0.398	71774	21.1
	20.815	4.2640	32029	0.317	12319	26.6
	21.180	4.1914	55626	0.38	25570	22.3
	22.278	3.9872	334152	0.445	180681	18.9
	26.950	3.3057	60216	0.535	34734	16.0
	29.501	3.0253	116994	0.378	51296	22.7
Ment-Gly	12.549	7.0479	41116	0.099	5120	84.0
	25.218	3.5285	314001	0.105	38853	80.8
	26.099	3.4115	527861	0.090	61006	94.4
Ment-Leu	6.853	12.889	117774	0.143	20567	57.9
	14.346	6.1689	17779	0.124	3655	67.3
	24.373	3.6491	22491	0.328	8209	25.9
Ment-His	20.130	4.4075	13204	0.129	2316	65.3
	22.341	3.9762	27486	0.135	5051	62.4
	22.996	3.8644	10361	0.159	2251	53.3
	25.889	3.4387	27084	0.144	4946	59.1
	26.464	3.3652	27905	0.119	5609	71.4
	30.821	2.8987	13105	0.2094	3136	41.1
	33.337	2.6855	11782	0.174	2448	49.7
	34.728	2.5810	8508	0.168	1832	51.9

16.8 g at 36 °C (F3), 31 g at 37–39 °C (F4), and 51.6 g at 42–50 °C (F5) with 18.5 g of residual oil remaining. The menthol crystals obtained from different fractions generally exhibited particles in the sub-micron to micron size range (200 nm–10 µm). The observation of a regular or semi-regular arrangement in many fractions (F1, F3, F4, F5, and residual oil) and in standard menthol crystals suggested a common trend in the crystal formation processes. The prevalence of rectangular-shaped particles and the presence of spaces between particles in many of the menthol samples were also another similarities. However, there were also distinct morphological differences between the fractions. The standard menthol crystals showed a unique accordion-like, folded sheet structure, which was not observed in the other fractions. The F1 fraction was distinguished by its smooth-surfaced and more distinctly rectangular nanoparticles, while the F2 fraction stood out with its rough-surfaced and semi-rectangular/cubic-like particles. In the F3 fraction, clustered needle-like structures were observed in addition to the regular arrangement. This diversity in the surface roughness and particle shapes indicated that different fractionation conditions significantly influenced the crystal growth processes and the resulting morphologies. Consequently, while there was a general trend in the crystal structures, each fraction exhibited its own unique microstructural features.

Figures 6 and 7 show SEM images of the menthol (a), Ment-Gly (b), Ment-Leu (c), and Ment-His (d) compounds at magnifications of × 10,000 and × 20,000, respectively. The SEM

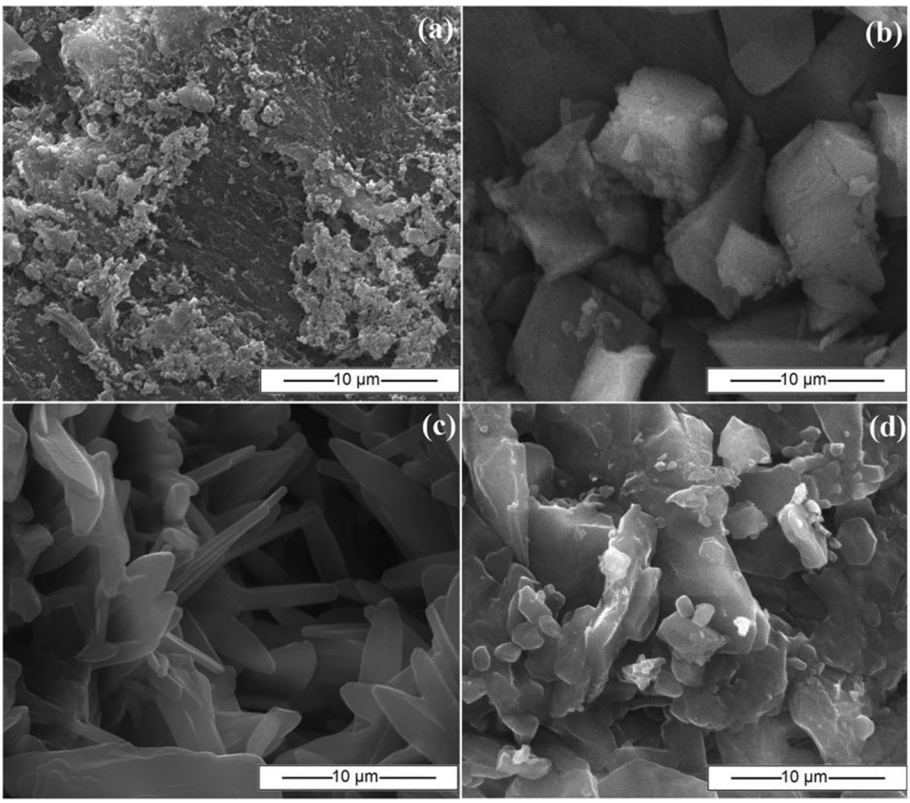

Fig. 6 SEM images (× 10,000) of the menthol (**a**), Ment-Gly (**b**), Ment-Leu (**c**), and Ment-His (**d**)

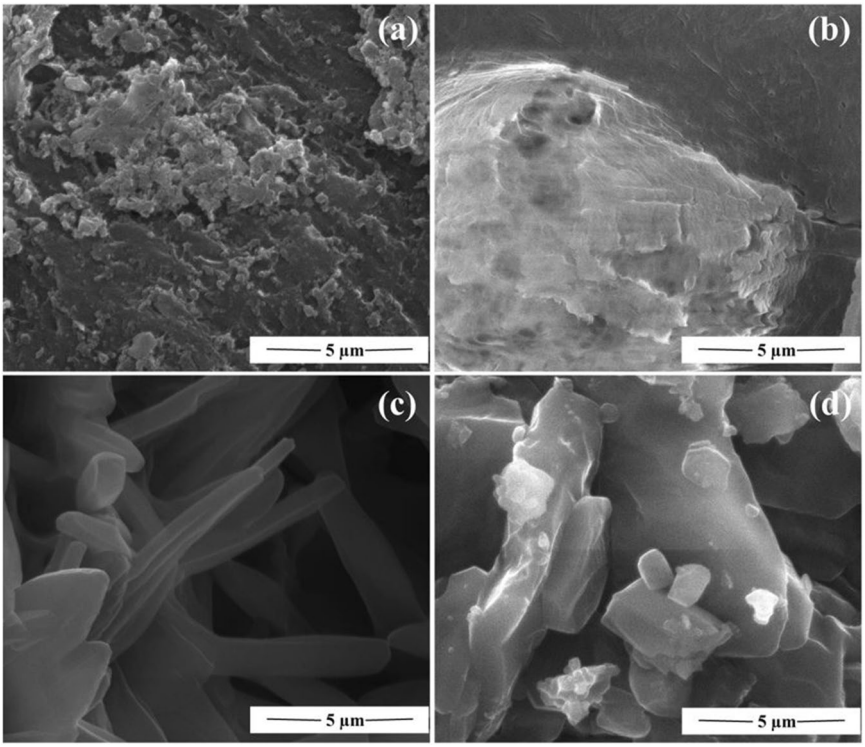

Fig. 7 SEM images (×20,000) of the menthol (**a**), Ment-Gly (**b**), Ment-Leu (**c**), and Ment-His (**d**)

images of the menthol (Figs. 6a and 7a) show clusters of irregularly shaped small particles ranging in size from sub-micrometers to several micrometers on its surface. This morphology is similar to that observed in another study [22]. The surface of Ment-Gly has irregular, angular particles with sharp edges and varying sizes (Fig. 6b) and non-uniform structures of the stacked layers in sub-micron size (Fig. 7b). The presence of rod-like and succulent leaf-like structures with lengths at microscale and thicknesses at nanoscale is seen on the surface of Ment-Leu in Figs. 6c and 7c. The large and small non-uniform structures from sub-micrometers to micrometers and the clusters of the small ones are observed in the SEM images of Ment-His compound (Figs. 6d and 7d). The SEM analyses revealed that the menthol compounds synthesized in this study are morphologically different from the menthol, and the size of the structures observed in the compounds is greater than that of the particles in the menthol.

MIC and MBC/MFC Values

The MIC and MBC/MFC values of the menthol and the menthol-amino acid derivatives for seven bacterial species and the fungus are shown in Figs. 8, 9, and 10. The findings in these figures show that all compounds exhibit antimicrobial activity against all microbial strains. It is observed that the lowest values belong to Ment-Leu and Ment-His compounds for *B. cereus*, when comparing the MIC values of the compounds for the Gram (+) bacteria in Fig. 8. In terms of MBC values, Ment-Gly and Ment-His have the lowest values for the same bacterium while the menthol has the lowest value for *S. agalactiae*. Lower MIC

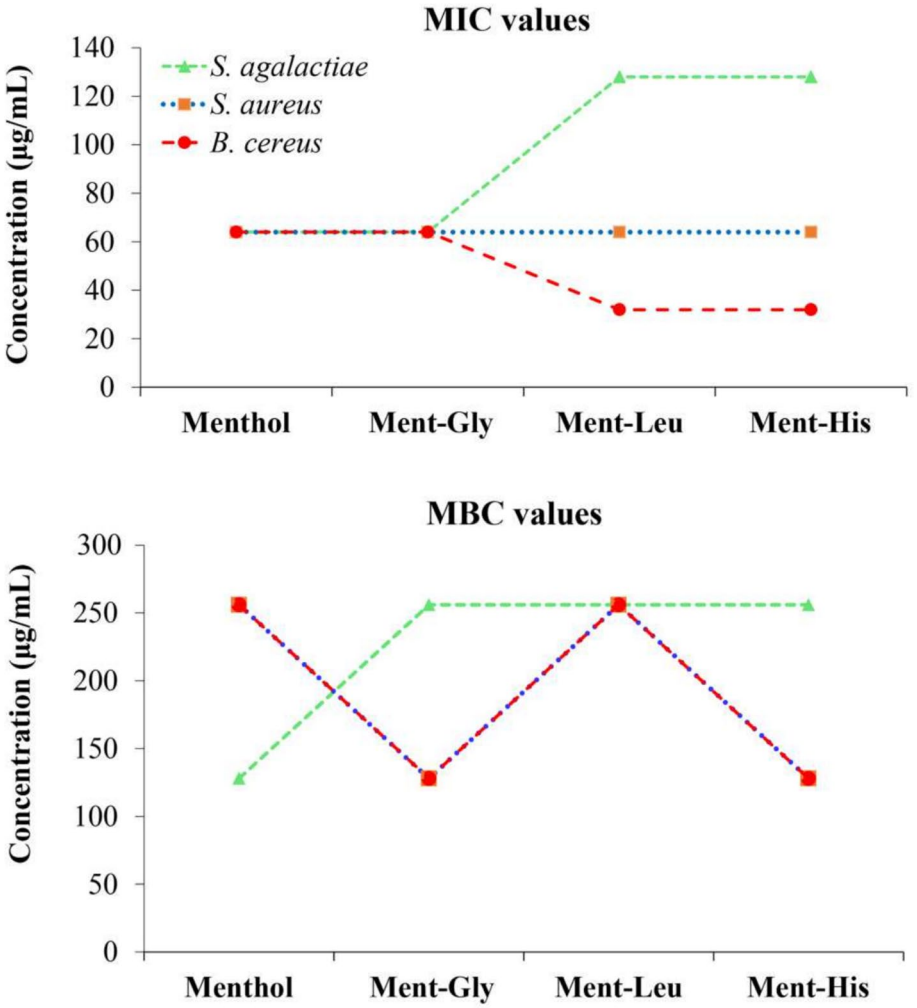

Fig. 8 MIC and MBC values of the compounds for the Gram (+) bacteria

and MBC values indicate higher potency of the agent. Thus, Ment-His has the most potent against *B. cereus* among the Gram (+) bacteria.

As seen in Fig. 9, the lowest MIC values belong to Ment-His for *P. vulgaris* and *K. pneumoniae* among the Gram (−) bacteria. Regarding the MBC values, the menthol and Ment-Gly have the lowest values *for S. marcescens* and *P. vulgaris*, respectively. Comparing the data in Figs. 8 and 9, all compounds are seen to be more effective against the Gram (+) bacteria than the Gram (−) ones. It was stated that Gram (+) bacteria were more sensitive to essential oils than Gram (−) bacteria [34]. The reason for this could be that Gram (−) bacteria having a hydrophilic outer membrane prevent the penetration of hydrophobic essential oils into the target cell membrane [35].

The MIC values of the menthol range from 64 to 128 µg/mL all bacterial species. Menthol disrupts membrane-associated properties, affecting the proton motive force essential for ATP synthesis and nutrient transport, thereby inhibiting microbial growth and survival

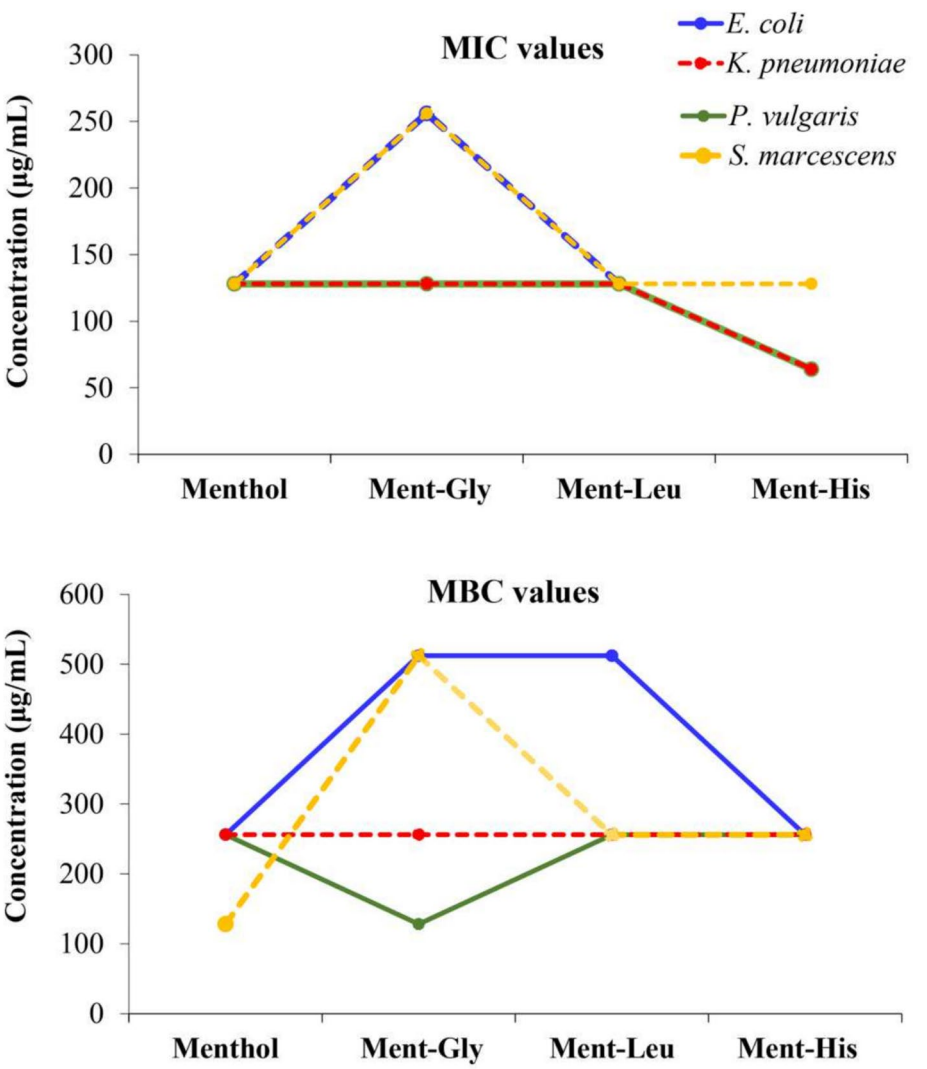

Fig. 9 MIC and MBC values of the compounds for the Gram (−) bacteria

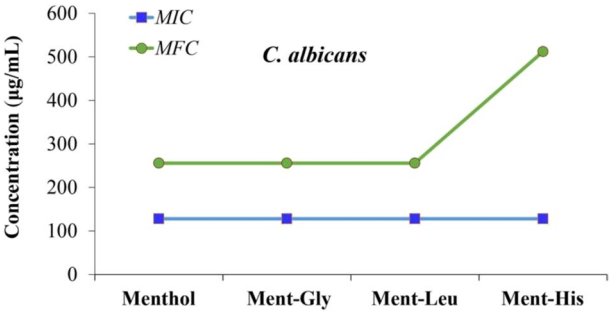

Fig. 10 MIC and MFC values of the compounds for the fungus

[36, 37]. Ment-Gly shows antimicrobial efficacy between MIC values of 64 and 256 µg/mL against all microbial strains, as seen in Figs. 8 and 9. It is observed that this compound is more effective (MIC 64 µg/mL) on *S. aureus*, *B. cereus*, and *S. agalactiae* than other microorganisms. Glycine inhibits the synthesis of peptidoglycan, an important component of the bacterial cell wall [38, 39]. In addition, it can cause lysis in certain bacteria, leading to morphological changes that increase their antimicrobial effects [40]. It is thought that the effect of Ment-Gly on the peptidoglycan layer increases the antimicrobial property. Ment-Leu and Ment-His exhibit an MIC range of 128–32 µg/mL for the microorganisms (Figs. 8 and 9). These compounds exhibit the strongest antimicrobial activity, with MIC value of 32 µg/mL against *B. cereus*. Torres et al. [41] stated that Leucine-added antimicrobial peptides and their modified compounds penetrated cell membranes, and exhibited broad-spectrum activity against both Gram (+) and Gram (−) bacteria, leading to cell lysis. It is seen that Ment-His is more effective against almost all Gram (−) and Gram (+) bacteria than other compounds (Figs. 8 and 9). When incorporated into lytic peptides, histidine enhances selectivity and efficacy against antibiotic-resistant bacteria by facilitating deeper membrane insertion. Additionally, these components form a potent antimicrobial complex that is effective against various bacterial strains [42]. Menthol-histidine compounds were also found to have antimicrobial activity through multiple mechanisms, primarily by targeting bacterial membranes and inhibiting virulence factors [36].

As seen in Fig. 10, the menthol and its compounds have the same MIC value of 128 µg/mL against *C. albicans*. With the exception of Ment-His compound (512 µg/mL), MFC values are the same for the other compounds (256 µg/mL). *C. albicans* is among the most extensively studied fungal species in relation to menthol. Menthol shows strong antifungal activity by affecting membrane integrity and inducing apoptosis. This effect is associated with inhibition of planktonic growth, biofilm formation, and hyphal development in this fungus. The fact that menthol disrupts membrane integrity and affects cellular signaling pathways [37] explains the effect of the menthol and its compounds on *C. albicans* at relatively low concentrations. Studies reported that menthol exhibits MIC values of 0.78–500 µg/mL and MFC values of 1.5–1000 µg/mL against *C. albicans* [7]. The values obtained in this study are within the ranges reported in the study.

In the study utilizing menthol-loaded nanostructured lipid carriers, MIC values were determined as 125 µg/mL and 250 µg/mL against Gram (+) bacteria *S. aureus* and *B. cereus*, respectively. These values were reported as 500 µg/mL against *E. coli* (Gram (−)) and 78 µg/mL against *C. albicans* [43]. Menthol and its compounds in this study exhibit better MIC values against these bacteria than those in the study.

Conclusion

This study includes the preparation of menthol-amino acid ester derivatives (Ment-Gly, Ment-Leu, and Ment-His) and their characterization via HPLC, FTIR, ^{13}C-NMR, XRD, SEM, and the broth dilution analyses. The comparison of R_f values and the retention times in the HPLC findings confirmed the formation of new menthol-based compounds. The FTIR and ^{13}C-NMR results validated the successful synthesis of the menthyl ester derivatives through the reactions between the menthol and the amino acids. The distinct peaks indicating nanoscale crystallite structures in all compounds were identified by the XRD analyses. Each ester derivative was found to have a unique crystal structure differing from that of the menthol, and their average crystallite sizes of the compounds were

greater than that of the menthol. SEM analyses revealed that the surfaces of all compounds exhibited different morphologies, including the structures with widths or thicknesses in the sub-micron range.

The antimicrobial activity studies demonstrated the effects of the menthol and its amino acid ester derivatives on various microorganisms. All compounds showed higher efficacy, particularly against Gram (+) bacteria. Among them, Ment-His was the most effective against nearly all tested Gram (−) and Gram (+) bacteria. Given the increasing prevalence of antibiotic-resistant strains among both Gram (+) and Gram (−) bacteria, along with the limited efficacy of current antifungal agents against *C. albicans*, there is a growing need to explore alternative antimicrobial strategies. The emergence of multidrug-resistant pathogens has underscored the urgent need for novel, broad-spectrum antimicrobial compounds. The menthol-amino acid derivatives, particularly Ment-His, can be considered promising candidates for innovative applications in antimicrobial therapies and related scientific disciplines after their resistance development, efficacy, and safety potentials are confirmed through in vivo studies.

Supplementary Information The online version contains supplementary material available at https://doi.org/10.1007/s12010-025-05336-8.

Acknowledgements The authors thank the Balıkesir University Science and Technology Research and Application Center (BUSTRAC) for the ^{13}C-NMR analyses and METU Central Laboratory for the XRD and SEM analyses.

Author Contribution L.E., U.A., A.E., and A.M.: designed the concept and study; L.E., R.B., and P.G.: acquisition, analysis, and interpretation of data; L.E. and R.B.: drafted the article; R.B.: data curation and writing-review and editing; L.E, U.A, A.E, R.B., P.G., and A.M.: final approval of the version to be submitted. All authors have read and agreed to the published version of the manuscript.

Data Availability The data used to support the findings of this study are available from the corresponding author upon request.

Declarations

Ethics Approval No ethical approval or informed consent was required for this study.

Consent for Publication Not applicable.

Conflict of interest The authors declare no competing interests.

References

1. Akerele, O. (1993). Summary of WHO guidelines for the assessment of herbal medicines. *Herbal Gram, 28*(13), 13–9.
2. Hamburger, M., & Hostettmann, K. (1991). 7. Bioactivity in plants: The link between phytochemistry and medicine. *Phytochemistry, 30*(12), 3864–3874.
3. Rates, S. M. K. (2001). Plants as source of drugs. *Toxicon, 39*(5), 603–613.
4. Chaachouay, N., & Zidane, L. (2024). Plant-derived natural products: A source for drug discovery and development. *Drugs and Drug Candidates, 3*(1), 184–207.
5. King, M. B. (1976). Transactions. *Institute of Chemical Engineers, 54*(1), 54–60.
6. Zhao, Y., Pan, H., Liu, W., Pang, Y., Gao, H., He, Q., Liao, W., Zeng, J., & Guo, J. (2023). Menthol: An underestimated anticancer agent. *Frontiers in Pharmacology, 14*, 1148790.
7. de Castro Teixeira, A. P., de Sousa Melo, F. M., Lima, I. O., de Luna Freire Pessôa, H., & de Cássia da Silveira e Sá, R. (2024). Do menthol and its derivatives present biological activity with antifungal potential? *Journal of Essential Oil Research, 36*(4), 291–320.

8. Ettibaeva, L. A., Abdurakhmanova, U. K., Matchanov, A. D., Allanazarova, D. M., & Halmuratova, Z. T. (2021). Influence of glycyrrhizic acid, menthol and their supramolecular compounds on the functional activity of rat mitochondria in in-vitro experiments. *Journal of the Korean Chemical Society, 65*(5), 313–320.
9. Ettibaeva, L. A., Abdurakhmanova, U. K., & Matchanov, A. D. (2023). Study of glycyrrhizic acid: Menthol supramolecular complexes on mitochondrial functional activity in in-vitro experiments. *Journal of the Korean Chemical Society, 67*(2), 99–105.
10. Deepalekshmi, P., Mahadevaprasad, B., Apoorva, S. N., Shreya, K., & Bettadaiah, B. K. (2023). A feasible synthesis of (−)-menthol-amino acid conjugates as potential TRPM8 agonists. *ChemistrySelect, 8*(42), e202303267.
11. Kamble, M., Sabale, P., Dhabarde, D., Sabale, V., & Mule, A. (2024). Synthesis of amino menthol derivatives for enhanced antimicrobial and anti-inflammatory activity using in-silico design. *Research Journal of Pharmacy and Technology, 17*(6), 2669–2675.
12. Takasawa, S., Kimura, K., Miyanaga, M., Uemura, T., Hachisu, M., Miyagawa, S., ... & Arimura, G. I. (2024). The powerful potential of amino acid menthyl esters for anti-inflammatory and anti-obesity therapies. *Immunology*, *173*(1), 76–92.
13. Tsuzuki, C., Hachisu, M., Iwabe, R., Nakayama, Y., Nonaga, Y., Sukegawa, S., Horito., S. & Arimura, GI. (2022). An amino acid ester of menthol elicits defense responses in plants, *Plant Molecular Biology, 109*(4-5), 523–531.
14. Huang, L., Chen, R., Luo, J., Hasan, M., & Shu, X. (2022). Synthesis of phytonic silver nanoparticles as bacterial and ATP energy silencer. *Journal of Inorganic Biochemistry, 231*, 111802.
15. Saif, M. S., Zafar, A., Waqas, M., Hassan, S. G., Haq, A., Tariq, T., Batool, S., Dilshad, M., Hasan, M., & Shu, X. (2021). Phyto-reflexive zinc oxide nano-flowers synthesis: an advanced photocatalytic degradation and infectious therapy. *Journal of Materials Research and Technology, 13*, 2375–2391.
16. Hasan, M., Zafar, A., Shahzadi, I., Luo, F., Hassan, S. G., Tariq, T., Zehra, S., Munawar, T., Iqbal, F., & Shu, X. (2020). Fractionation of biomolecules in Withania coagulans extract for bioreductive nanoparticle synthesis, antifungal and biofilm activity. *Molecules, 25*(15), 3478.
17. Hussain, R., Hasan, M., Iqbal, K., Zafar, A., Tariq, T., Saif, M. S., Hassan, S. G., Shu, X., Caprioli, G., & Anjum, S. (2023). Nano-managing silver and zinc as bio-conservational approach against pathogens of the honey bee. *Journal of Biotechnology, 365*, 1–10.
18. Hasan, M., Liu, Q., Kanwal, A., Tariq, T., Mustafa, G., Batool, S., & Ghorbanpour, M. (2024). A comparative study on green synthesis and characterization of Mn doped ZnO nanocomposite for antibacterial and photocatalytic applications. *Scientific Reports, 14*(1), 7528.
19. Clinical and Laboratory Standards Institute (CLSI) (2018). Standard M07 Methods for Dilution Antimicrobial Susceptibility Tests for Bacteria That Grow Aerobically, 11th ed., Wayne, PA.
20. Clinical and Laboratory Standards Institute (CLSI) (2017). Standard M27 Refences Methods for Broth Dilution Antifungal Susceptibility Testing of Yeasts, 4th ed., Wayne, PA.
21. Pätzold, M., Burek, B. O., Liese, A., Bloh, J. Z., & Holtmann, D. (2019). Product recovery of an enzymatically synthesized (−)-menthol ester in a deep eutectic solvent. *Bioprocess and Biosystems Engineering, 42*, 1385–1389.
22. Mushtaq, A., Hanif, M. A., Nadeem, R., & Mushtaq, Z. (2024). Development of methodology for molecular crystallization of menthol. *Heliyon, 10*, e38394.
23. Madrigal-Trejo, D., Villanueva-Barragán, P. S., Zamudio-Ramírez, R., Cervantes-de la Cruz, K. E., Mejía-Luna, I., Chacón-Baca, E., ... & Heredia-Barbero, A. (2021). Histidine self-assembly and stability on mineral surfaces as a model of prebiotic chemical evolution: an experimental and computational approach. *Origins of Life and Evolution of Biospheres*, *51*(2), 117–130.
24. Kumar, M. A., & Selvam, P. (2016). Amino-functionalized phosphotungstic acid-anchored mesoporous molecular sieves: Highly efficient catalysts for selective epoxidation of cyclohexene. *Advanced Porous Materials, 4*(2), 110–117.
25. Pathreeker, S., & Hosein, I. D. (2022). Vinylimidazole-based polymer electrolytes with superior conductivity and promising electrochemical performance for calcium batteries. *ACS Applied Polymer Materials, 4*(10), 6803–6811.
26. Silverstein, R. M., Webster, F. X. & David, J. K. (2005). In Infrared and Raman Characteristic Group Frequencies (Eds.: J. Yee), State University of New York, p. 487.
27. Härtner, J., & Reinscheid, U. (2008). Conformational analysis of menthol diastereomers by NMR and DFT computation. *Journal of Molecular Structure,* 872, 145–149.
28. Raikova, T. S., Kalechits, G. V., Manukov, E. N., Vyalimyae, T. K., & Makhach, S. A. (1981). Synthesis and structure of amino esters of menthol. *Chemistry of Natural Compounds, 17*, 526–530.

29. Frey, M. H., & Opella, S. J. (1986). The Effect of pH on solid-state 13C NMR spectra of histidine. *Journal of Magnetic Resonance, 66*(1), 144–147.
30. Wright, F. E. (1917). The crystallization of menthol. *Journal of the American Chemical Society, 39*(8), 1515–1524.
31. Corvis, Y., Négrier, P., Massip, S., Leger, J. M., & Espeau, P. (2012). Insights into the crystal structure, polymorphism and thermal behavior of menthol optical isomers and racemates. *CrystEngComm, 14*(20), 7055–7064.
32. Štejfa, V., Bazyleva, A., Fulem, M., Rohlíček, J., Skořepová, E., Růžička, K., & Blokhin, A. V. (2019). Polymorphism and thermophysical properties of l- and dl-menthol. *The Journal of Chemical Thermodynamics, 131*, 524–543.
33. Trivedi, M. K., Patil, S., Mishra, R. K., & Jana, S. (2015). Structural and physical properties of biofield treated thymol and menthol. *Molecular Pharmaceutics & Organic Process Research, 3*(2), 1000127.
34. Mann, C. M., Cox, S. D., & Markham, J. L. (2000). The outer membrane of Pseudomonas aeruginosa NCTC 6749 contributes to its tolerance to the essential oil of Melaleuca alternifolia (tea tree oil). *Letters in Applied Microbiology, 30*, 294–297.
35. Al-Bayati, F. A. (2009). Isolation and identification of antimicrobial compound from Mentha longifolia L. leaves grown wild in Iraq. *Annals of Clinical Microbiology and Antimicrobials, 8*, 20.
36. Tadevosyan, S., & Sahakyan, N. (2024). Influence of menthol on membrane-associated properties of tetracycline-resistant Escherichia coli. *AIMS Biophysics, 11*(3), 329–339.
37. Zore, G. B., Thakre, A. D., Abdulghani, M., Bhosle, K. H., Shelar, A., Patil, R., Kharat, K. R., & Karuppayil, S. M. (2022). Menthol inhibits candida albicans growth by affecting the membrane integrity followed by apoptosis. *Evidence-based Complementary and Alternative Medicine*. Article ID 1297888.
38. Gillissen, G., Schumacher, M., & Breuer-Werle, M. (1991). Modulation of antimicrobial effects of beta-lactams by amino acids in vitro. *Zentralblatt Für Bakteriologie, 275*(2), 223–232.
39. Sahal, G., Akan, H. S., & Karaca, T. D. (2024). Antimicrobial, antibiofilm and anticancer potentials of glycine and glycyl-glycine; an in vitro study. *Hacettepe Journal of Biology and Chemistry, 52*(4), 273–283.
40. Giordano, C., & Barnini, S. (2024). Glycine restores the sensitivity to antibiotics in multidrug-resistant bacteria. *Microbiology Spectrum, 12*, e00164-24.
41. Torres, M. D. T., Pedron, C. N., da Silva Lima, J. A., da Silva, P. I., da Silva, F. D., & Oliveira, V. X. (2017). Antimicrobial activity of leucine-substituted decoralin analogs with lower hemolytic activity. *Journal of Peptide Science, 23*(11), 818–823.
42. Kharidia, R., Tu, Z., Chen, L., & Liang, J. F. (2012). Activity and selectivity of histidine-containing lytic peptides to antibiotic-resistant bacteria. *Archives of Microbiology, 194*(9), 769–778.
43. Piran, P., Kafil, H. S., Ghanbarzadeh, S., Safdari, R., & Hamishehkar, H. (2017). Formulation of menthol-loaded nanostructured lipid carriers to enhance its antimicrobial activity for food preservation. *Advanced Pharmaceutical Bulletin, 7*(2), 261–268.